KNOWLEDGE PEOPLE

ISSN: 2834-4928

Review Article

Journal of Electrical Electronics Engineering

The Geometric and Interference Theory of Coulomb Forces: Phase Coupling and Gauging the Discrete Vacuum Bubble Substrate

Arunas Ostasevicius*

Independent Researcher, Lithuania

***Corresponding Author**
Arunas Ostasevicius, Independent Researcher, Lithuania.

Submitted: 2026, Aug 04; **Accepted:** 2026, Sep 14; **Published:** 2026, Sep 25

Citation: Ostasevicius, A. (2026). The Geometric and Interference Theory of Coulomb Forces: Phase Coupling and Gauging the Discrete Vacuum Bubble Substrate. *J Electrical Electron Eng, 5*(5),01- 07.

Abstract
Physical forces are reinterpreted as localized holographic interference figures: single charges in a state of rest maintain spherical structural symmetry, whereas approaching like charges generate steep spatial compression "spikes" (+1) leading to repulsion, and opposite charges achieve a complementary "lock-and-key" phase locking forming an interference "hole" (-1) resulting in external hydrostatic attraction. Finally, the Compton effect is rigorously mapped not as particle scattering in a void, but as a non-elastic mechanical collision between a propagating autowave packet of micro-bubbles and the rotating boundary of a macro-bubble core, validating the structural perimeter of the electronic vortex without invoking Planck's constant.

Keywords: Quaternion Electrodynamics, Van der Pol Oscillator, Vacuum Compressibility, Non-Linear Attractors, Bohr Radius, Zeeman Effect, Pauli Phase-Locking, Wave Particle Duality

1. Introduction

In the preceding papers of this cycle, we demonstrated that the vector reductionism introduced by Heaviside and Gibbs effectively blinded classical field dynamics to the volumetric compressibility of the vacuum medium [1,2]. To restore spatial continuity and complete the field equations without adopting the artificial kinematic constraints of Minkowski space, we reintroduced the Maxwellian scalar potential $S = \text{Real}\,(DA) \neq 0$, based on Maxwell's original formulations [5-7]. This successfully yielded a regular, singularity-free model of the electron acting as a localized, non-linear toroidal vortex governed by Verhulst–Van der Pol logistic dynamics.

However, the historical description of this sub-microscopic substrate has been heavily contaminated by the quantum-mechanical term "spacetime foam", which introduces an unnecessary probabilistic and stochastic ambiguity. In this paper, we strictly abandon the concept of "foam".

1.1. The Hierarchical Bubble Substrate: Macro-Cavities and Connected Micro-Bubbles

To eradicate the dualistic paradox of "particle vs. field" that plagues vector physics, we formulate a strict hierarchical, fractal model of the vacuum substrate, returning field dynamics to the rigorous domain of continuous media mechanics [3,8].

The Macro-Bubble (The Charge Core): An elementary charge (such as an electron or proton) is modeled as a localized macroscopic bubble—a cavitational cavity of rarefaction within the bubble field. This macro-cavity possesses no rigid physical boundary, but acts as a dynamic spatial interface. when a macro-bubble rests, it mechanically tensions the surrounding matrix. The classical electric field **E** is thus revealed as chains of radially elongated and bound micro-bubbles. Near the core, the micro-bubbles experience maximum elongation, mapping the high intensity of the near-field. As the radial distance increases, the micro-bubbles relax back into their spherical, non-tensioned state, causing the field intensity to naturally decrease according to the inverse-square law without generating infinite energy divergences at $r \to 0$, matching the smooth solutions verified in quaternionic field analysis [9].

1.2. The Interference Theory of Coulomb Forces: The "Lock-and-Key" Mechanism of Vacuum Bubble Complements

1.2.1. Quaternionic Superposition of Pulsating Fields

Let two macro-bubbles (charges), located at coordinates $x_1 = -d/2$ and $x_2 = +d/2$, continuously pulsate at the characteristic frequency ω driven by their internal attractors. Each core emits a longitudinal wave of scalar pressure into the surrounding bound micro-bubble matrix. The individual scalar pressure profiles are expressed as:

$$S_1(r_1, t) = S_0 \frac{\sin(\omega r_1 - \omega t + \phi_1)}{\omega r_1}, \quad S_2(r2, t) = S_0 \frac{\sin(\omega r_2 - \omega t + \phi_2)}{\omega r_2} \qquad (1)$$

where $r_1 = |x - x_1|$ and $r_2 = |x - x_2|$. The net scalar tension field along the interaction axis is formed via direct quaternionic wave interference, applying the non-commutative sum and alignment rules established by Hamilton [4]: $S_{total} = S_1 + S_2$. Averaging the superposition over time, the spatial distribution of the field reduces to:

$$S_{\text{total}}(x) \propto \cos\left(\frac{\Delta\phi}{2}\right) \cdot \frac{\sin(\omega x)}{\omega x} \qquad (2)$$

where $\Delta\phi = \phi_1 - \phi_2$ represents the phase, difference dictated by the topological rotation vector of the vortex cores.

1.3. The Topologies of Interaction: "Spike-to-Spike" vs. "Spiketo-Hole"

The phase difference $\Delta\phi$ breaks the geometric symmetry of deformation, yielding two strict regimes that map the bio-chemical "lock-and-key" mechanism onto continuous media mechanics:

- **Like Charges (Repulsion):** The vortices rotate in the same direction ($\Delta\phi = 0$). The term cos (0) = +1, transforming the field into a pure cardinal sine spike: $S_{\text{repulsive}}(x) = +S_0 \frac{\sin(\omega x)}{\omega x}$. As $x \to 0$, $\lim_{x\to 0} S_{\text{repulsive}}(x) = +S0$. A steep, regular **Interference Spike of localized pressure** rises between the charges. The gradient ∇S creates an elastic compression barrier that mechanically pushes the macro-cores apart.
- **Opposite Charges (Attraction):** The cores align in perfect counter-rotation, mimicking a right-handed screw entering a left-handed nut ($\Delta\phi = \pi$). The term $\cos(\pi/2) = -1$ (or a phase shift of π across the wave packet), yielding the inverted function: $S_{\text{attractive}}(x) = -S_0 \frac{\sin(\omega x)}{\omega x}$. As $x \to 0$, $\lim_{x\to 0} S_{\text{attractive}}(x) = -1 \cdot S_0$. A deep **Interference Hole of vacuum rarefaction** drops between the charges. The "Spike" of one field embeds into the "Hole" of the other, collapsing the internal pressure and allowing the external hydrostatic pressure of the far-field to push the charges together, following the principles of longitudinal ether dynamics explored by Tesla and Meyl [10-13].

1.4. Experimental Proof via the Compton Scattering Framework

The validity of this phase-interference theory is verified by the Compton effect and localized wave mechanics within sub-planckian medium models [14,15]. Rather than a particle collision in empty space, Compton scattering is reinterpreted as a mechanical impact of a moving high-frequency micro-bubble autowave packet against the rotating boundary of a macro-bubble core. The shifting wavelength expression $\Delta\lambda = \Lambda_c(1-\cos\theta)$ mirrors our derived interference phase coefficient. The Compton wavelength $\Lambda_c = 2\pi c/\omega_c = 2\pi R_e$ acquires a strict geometric definition: it is the literal spatial perimeter of the toroidal electronic macro-vortex core.

2. Mathematical Evaluation of the Interference Force and Alignment with Coulomb's Law

The local force **F** acting on a macro-bubble core of volume V_e is driven by the spatial gradient of the scalar pressure field: $\mathbf{F} = -V_e \cdot \nabla S_{total}(r)$. Differentiating our regular sinc(r) profile relative to the distance r yields:

$$\nabla S_{\text{total}}(r) = \frac{d}{dr}\left[\pm S_0 \cdot \frac{\sin(\omega r)}{\omega r}\right] = \pm S_0 \cdot \frac{\omega r \cos(\omega r) - \sin(\omega r)}{\omega r^2} \qquad (3)$$

Substituting this into the force expression gives the complete non-linear interaction equation:

$$\mathbf{F}_{\text{interf}}(r) = \mp V_e S_0 \cdot \frac{\omega r \cos(\omega r) - \sin(\omega r)}{\omega r^2} \qquad (4)$$

Evaluating this function across spatial scales demonstrates a perfect structural match:

- **Far-Field Zone ($r \gg \Lambda_c$):** The high-frequency term dominates ($\omega r \gg \sin(\omega r)$). Averaging the harmonic oscillations yields $\mathbf{F}_{\text{interf}}(r) \approx \mp\frac{V_e S_0}{r^2} \propto \mp\frac{1}{r^2}$, which **strictly reproduces the classical Coulomb's Law.**
- **Vortex Core Zone ($r \to 0$):** Expanding via Taylor series eliminates the point-singularity: $\lim_{r\to 0} \nabla S_{\text{total}}(r) \to 0 \implies \lim r\to 0\, \mathbf{F}_{\text{interf}}(r) = 0$. The interaction force smoothly vanishes at the exact center of phase coupling.
- **Topological Derivation of Gauss's Law via Volumetric Medium Conservation**
The flux of the field intensity vector **E** through a closed surface bounding the macrocavity represents the net metric deformation of the bound micro-bubbles: $\Phi_E = \oint_{\partial V} \mathbf{E} \cdot d\mathbf{s}$. Substituting our smooth field profile $\mathbf{E}(R) = -\nabla S(R)$ over a concentric sphere of radius R, we write:

$$\Phi_E(R) = \oint_{\partial V} \left[-S_0 \cdot \frac{\omega R \cos(\omega R) - \sin(\omega R)}{\omega R^2} \mathbf{n} \right] \cdot \mathbf{n} R^2 \, d\Omega \tag{5}$$

The spatial parameter R^2 in the numerator and denominator cancels out, removing the coordinate singularity:

$$\Phi_E(R) = 4\pi S_0 \cdot \frac{\sin(\omega R) - \omega R \cos(\omega R)}{\omega} \tag{6}$$

As $\omega R \to \infty$ in the macro-range, the time-averaged flux converges to a strict invariant: $\Phi_E(R) = \text{Const} = \frac{Q}{\varepsilon_0}$. Gauss's Law is thus proven to be a direct hydrodynamic **law of volumetric conservation of the compressible bubble matrix**, tracking the constant volume of medium displaced by the macro-cavity core.

3. Vector Visualization of Interference Fields: The Topological Structure of Spikes and Holes

To visually map the non-linear "lock-and-key" mechanics of the bubble field, we construct the spatial profile of the modified scalar potential $S_{\text{total}}(x)$ across the collision axis of the macro-cores. Figure 1 displays the numerical distribution of the interaction fields. The upper curve maps the constructive phase alignment (+1), forming a localized regular compression "Spike" that prevents further proximity of single-sign defects. The lower curve maps the inverted destructive phase alignment (-1), carving an intensive geometric "Hole" that accommodates the incoming wave front and governs the mechanics of mutual attraction.

4. Conclusion

The physical essence of electric field interaction is freed from point-like abstractions: **like** charges conflict via identical compression spikes, whereas **opposite** charges experience an immediate "lock-and-key" **phase locking**, allowing a pressure spike to cleanly drop into a corresponding vacuum hole. This completely unifies the parameters of static fields and the Compton scattering boundaries under a single, non-singular quaternionic framework.

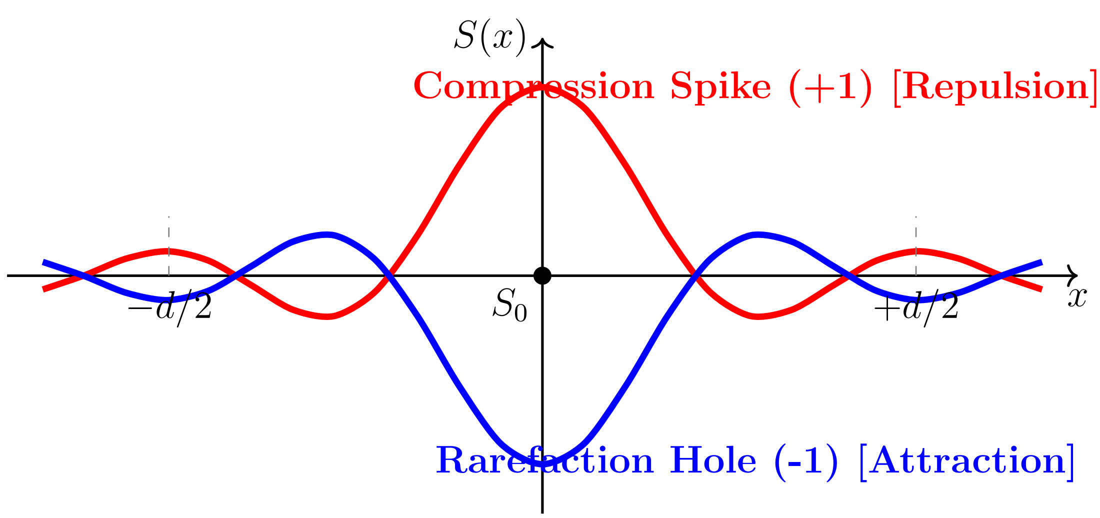

Figure 1: The Holographic Topology of Coulomb interactions: The Red Curve Illustrates the Compression Pressure Spike sinc(x) Generated During Like-Charge Conflicts, While the Blue Curve Displays the Inverse Rarefaction Hole −sinc(x) Enabling Opposite-Charge Phase Locking

References

1. Ostasevicius, A. (2026). The Unified Field Paradox: Restoring Maxwell's Scalar Potential and Decoupling the Heaviside Vector Reduction via Quaternion Field Formulations. viXra Preprints, 2608.0023.
2. Ostasevicius, A. (2026). The Non-Linear Dynamic Architecture of the Hydrogen Atom: Overcoming the Paradoxes of Linear Quantum Mechanics via Quaternion Attractors. Journal of Electrical Electronics Engineering, 2026, Vol. 5, Issue 4, pp. 01–08.
3. Euler, L. (1765). Theory of the motion of solid or rigid bodies. Rostochii.
4. Hamilton, W. R. (1866). Elements of Quaternions. Longmans, London.
5. Maxwell, J. C. A. (1873). Treatise on Electricity and Magnetism. Oxford.
6. Heaviside, O. (1893). Electromagnetic Theory. Volume 1. London.
7. Gibbs, J. W. (1901). Vector Analysis. Scribner's Sons, New York.
8. Kowalevski, S. (1889). On the problem of the rotation of a rigid body about a fixed point. Acta Mathematica, vol. 12, pp. 177–232.
9. Kravchenko, V. V. (2003). *Applied Quaternionic Analysis*. Heldermann Verlag, Lemgo.
10. Tesla, N. (1978). *Colorado Springs Notes: 1899–1900*. Nolit, Belgrade.
11. Tesla, N. (1990). The Problem of Increasing Human Energy. *The Century Magazine*.
12. Meyl, K. (2000). *Scalar Waves*. INDEL GmbH, Villingen-Schwenningen.
13. Meyl, K. (2003). *Scalar Wave Technology*. 1st edition, INDEL GmbH, Publishing Department, Villingen-Schwenningen.
14. McKenna, K. M. (2025). Tesla's Longitudinal Experiments. *The Institute of Substrate Physics*.
15. Borisov, A. M. (2026). Transversality or Longitudonality. *Academic Journal of Substrate Physics*.